Multispectral and Photoplethysmography Optical Imaging Techniques Identify Important Tissue Characteristics in an Animal Model of Tangential Burn Excision

Jeffrey E. Thatcher, PhD,* Weizhi Li, MS,* Yolanda Rodriguez-Vaqueiro, PhD,† John J. Squiers, BSE,*‡ Weirong Mo, PhD,* Yang Lu, PhD,* Kevin D. Plant, BS,* Eric Sellke, BS,* Darlene R. King, BS,* Wensheng Fan, MS,* Jose A. Martinez-Lorenzo, PhD,† and J. Michael DiMaio, MD*‡

Burn excision, a difficult technique owing to the training required to identify the extent and depth of injury, will benefit from a tool that can cue the surgeon as to where and how much to resect. We explored two rapid and noninvasive optical imaging techniques in their ability to identify burn tissue from the viable wound bed using an animal model of tangential burn excision. Photoplethysmography (PPG) imaging and multispectral imaging (MSI) were used to image the initial, intermediate, and final stages of burn excision of a deep partial-thickness burn. PPG imaging maps blood flow in the skin's microcirculation, and MSI collects the tissue reflectance spectrum in visible and infrared wavelengths of light to classify tissue based on a reference library. A porcine deep partial-thickness burn model was generated and serial tangential excision accomplished with an electric dermatome set to 1.0 mm depth. Excised eschar was stained with hematoxylin and eosin to determine the extent of burn remaining at each excision depth. We confirmed that the PPG imaging device showed significantly less blood flow where burn tissue was present, and the MSI method could delineate burn tissue in the wound bed from the viable wound bed. These results were confirmed independently by a histological analysis. We found these devices can identify the proper depth of excision, and their images could cue a surgeon as to the preparedness of the wound bed for grafting. These image outputs are expected to facilitate clinical judgment in the operating room. (J Burn Care Res 2016;37:38–52)

Sharp tangential excision is the partial excision of a burn in a uniform, serial fashion until the viable wound bed is reached.[1] Surgical excision is necessary in severe burns that are classified as either deep partial thickness or full thickness, because these burns have eliminated the skin's regenerative capacity. Excision and grafting allows healing and prevents necrosis, contractures, disfiguring scarring, and other complications that, without surgery, ultimately lead to amputation, death, or other comorbidities.[2]

One of the most challenging aspects during excision is the delineation of vital from nonvital tissue. Important features of the tissue that differentiate injury from healthy wound beds were described as early as 1953 by Jackson.[3] In this three-zone model, blood flow, inflammation, and protein denaturation are important differentiating features. Yet none of these features can be easily assessed quantitatively during surgery. The current gold standard histology is slow and does not translate easily to irregular depth of burn often seen in the clinical setting; blood flow can be seen during surgery, but only after excision. Diagnostic imaging tools that measure perfusion are available, such as laser Doppler imaging and

*From *Spectral MD, Inc., Dallas, Texas; †Department of Electrical and Computer Engineering, Northeastern University, Boston, Massachusetts; and ‡Baylor University Medical Center, Dallas Texas.*

J.E.T., W.F., and J.M.D. receive salary from Spectral MD and have ownership in Spectral MD, Inc. through stock. K.D.P. has ownership in Spectral MD, Inc. through stock.

Address correspondence to Jeffrey Thatcher, PhD, Spectral MD, Inc., 2515 McKinney Ave. Ste. 1000 Dallas, Texas 75201. E-mail: thatcher@spectralmd.com.

1559-047X/2015

DOI: 10.1097/BCR.0000000000000317

indocyanine green imaging, but these tools can be costly and require significant training.[4]

Histological staining of excised burn eschar has shown that up to half of the tissue removed during a burn surgery is actually viable.[5] It is unknown how often surgeons excise deeper than necessary, but at least one study has demonstrated that the majority of sharp tangential excisions performed resect well into the underlying viable tissue.[5] Unnecessary excision into viable tissue has been explained by the difficulty in estimating burn depth, the inconsistency of burn depth across the injured area, and the expertise needed to attain a skillful clinical judgment.[6–9] These data are not validated across the country, and no standard has been established to rate excessive excision. It is clear, however, that both burn depth assessment and the proper depth of excision are difficult to identify with clinical judgment alone,[9] and that years of training are necessary to develop these skills. Nonsurgical burn debridement methods, such as enzymatic or chemical, retain more viable tissue, but they are slow and expose the patient to the risk of infection. Therefore, the present consensus is that a tool to aid a surgeon in rapidly and quantitatively identifying the proper depth of sharp tangential excision and/or burn severity over a large tissue surface area would be of value.

To address the possibility of improving the accuracy of sharp tangential excision, we explored two rapid and noninvasive optical imaging techniques in an animal model of burn excision: photoplethysmography imaging (PPG imaging) and multispectral imaging (MSI) (Figure 1). PPG imaging is a perfusion measurement that detects the intensity of arterial blood flow just below the surface of the skin.[10] MSI analyzes the various wavelengths of light absorbed and reflected by tissues to classify tissue by comparing its investigated reflectance spectra to a reference library. There are a variety of other technologies that have been proposed to aid the burn surgeon, including laser Doppler imaging, indocyanine green imaging, color photography, hyperspectral imaging, and thermography.[4,6,11,12] We chose to investigate PPG imaging and MSI modalities because they complement each other in the type of tissue properties they assess, and they can be performed using the same hardware. Our objective was to determine whether these technologies could distinguish burn tissue from viable tissue at multiple stages of sharp tangential excision in an animal model.

PHOTOPLETHYSMOGRAPHY IMAGING

PPG imaging is the same technology used in pulse oximetry to capture vital signs including heart rate, respiratory rate, and SpO_2.[13] The PPG

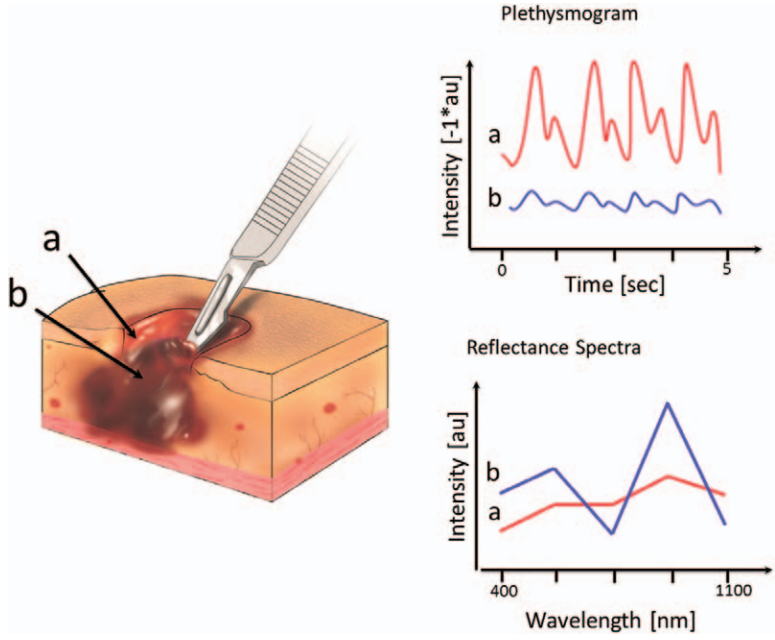

Figure 1. During burn excision procedures, the viable wound bed for grafting (A) is exposed by removing necrotic tissue (B). The photoplethysmography (PPG) imaging device detects the difference in relative blood flow to distinguish one tissue from the other. Meanwhile, multispectral imaging (MSI) technology can differentiate these tissues using the reflectance spectra determined by the molecular and structural difference between the wound bed (A) and necrotic burn tissue (B).

signal is generated by measuring light's interaction with dynamic changes in the vascularized tissues (Figure 2). Vascularized tissue expands and contracts in volume by approximately 1 to 2% with each incoming systolic blood pressure wave at the frequency of the cardiac cycle.[14] This influx of blood not only increases the volume of the tissue, but it also brings additional hemoglobin proteins that strongly absorb light. Therefore, the absorbance of light within the tissue oscillates with each heartbeat. Changes in tissue blood flow can thereby be identified by analyzing the plethysmogram generated by recording how light is absorbed as it travels through tissue. This information is then translated into the vital signs reported by pulse oximeters.

To generate images from the plethysmogram, we take advantage of the light's pathway through the tissues.[15] A small portion of light incident on the tissue surface scatters into the tissue. A fraction of this scattered light exits the tissue from the same surface it initially entered.[16] Using a sensitive digital camera, this back-scattered light is collected across an area of tissue so that each pixel in the imager contains a unique PPG waveform determined by changes in intensity of the scattered light. To generate a two-dimension (2D) map of relative tissue blood flow, the amplitude of each unique waveform is measured. To improve accuracy, we can measure the average amplitude over many heart beat samples.

MULTISPECTRAL IMAGING

MSI measures the reflectance of select wavelengths of visible and near-infrared light from a surface (Figure 3). Spectral characterization of substances is primarily used in remote sensing (eg, satellite or inflight imaging) for geological exploration or the detection of military targets but is gaining ground in medical applications.[17] MSI is applicable to burns because various tissue types, including both viable and necrotic tissue, consist of a unique combination of tissue components that interact with light differently. These varied light-tissue interactions produce unique reflectance signatures that are captured by MSI.[18] Spectral signatures collected from a patient's burn are compared with a database of known spectral signatures to characterize the patient's burn. Although MSI has lower number of unique wavelengths to describe the tissue compared with newer hyperspectral imagers, MSI remains superior when the combination of spatial resolution, spectral range, image acquisition speed, and cost are considered.[17]

Spectral identification of burn severity has been proposed as a means to supplement clinical observation during initial burn assessment as early as the 1970s.[19] The feasibility of identifying burn severity by studying unique optical reflectance properties of burns of differing depth was demonstrated in 1977 using a National Aeronautics and Space Administration–developed camera equipped with interchangeable

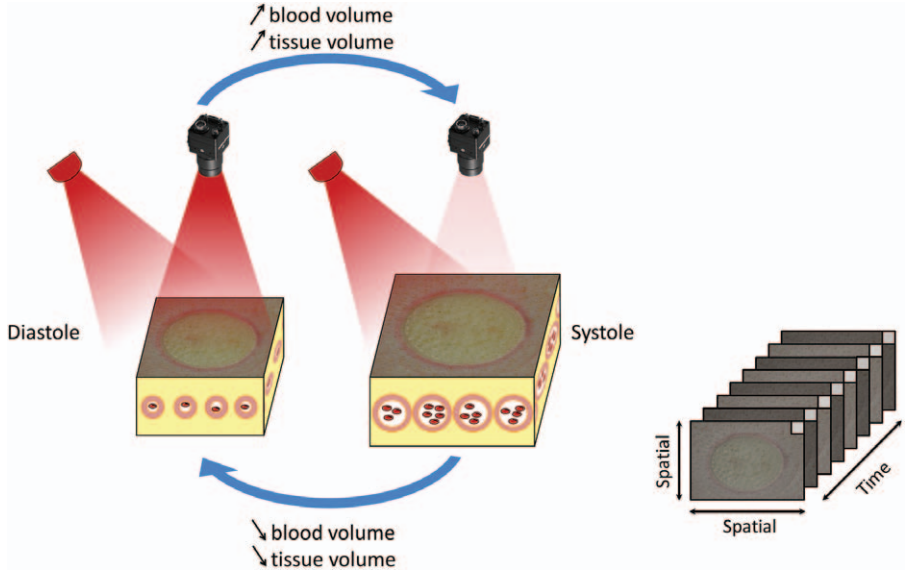

Figure 2. The major components of our reflectance mode and two-dimensional photoplethysmography (PPG) imaging system (left). Monochromatic light incident on the tissue surface scatters within the tissue as it interacts with molecular structures. A small portion of that light returns to the camera. When measured over time, the intensity changes in the back-scattered light produce a PPG waveform. Each pixel in the raw data cube contains a unique PPG waveform that is analyzed to generate a single blood flow image of the tissue (right).

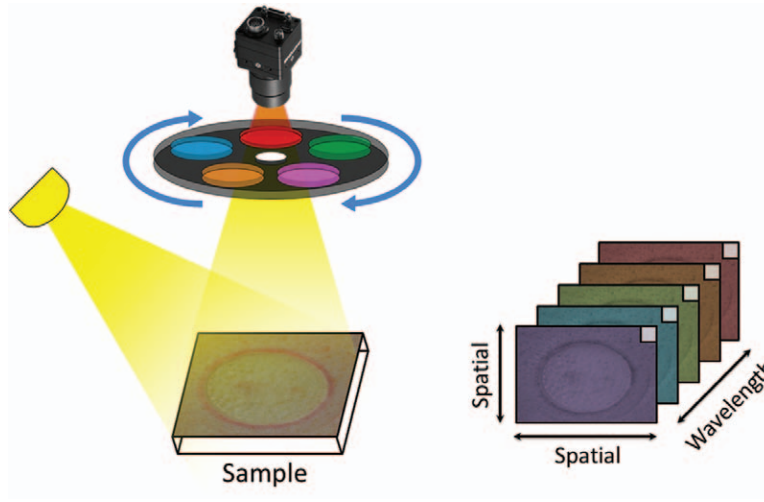

Figure 3. The major components of our multispectral imager included a broad spectrum illumination source, a digital camera, and a rotating filter wheel equipped with various optical filters that isolate predetermined wavelengths of light reflected from the target's surface (left). This system quickly collects an image at each position in the filter wheel to generate a spectral data cube (right). Each pixel in the data cube represents a low spectral-resolution reflectance spectrum of the tissue.

filters.[19] Other groups also achieved some success in applying this technology to characterize burn tissues.[20,21] They not only showed that MSI was capable of improved determination of burn depth when compared with clinical judgment, but also reported MSI was limited in clinical applications by technical difficulties such as the need to filter increasingly bright spectral reflection from the moisture on the skin's surface. Most importantly, MSI required data acquisition times on the order of days when this technology was initially developed because of severe limitation in data processing that engineers no longer face today given modern computing technology. More recently, our group has assessed the use of MSI in differentiating key burn tissues, including various burn depths.[22,23]

OVERVIEW

To apply PPG imaging and MSI technologies to burn care, scientists and engineers must demonstrate the ability of these technologies to improve the current standard of care. In this article, we outline our experiments to determine whether these technologies could distinguish burn tissue from viable tissue at multiple stages of sharp tangential excision in an animal model. PPG imaging was used to determine whether blood flow variations could distinguish viable tissue from nonviable. For MSI imaging, a spectral reference library was developed from an animal image database composed of images taken from known time points during burn excision and used to train a supervised machine-learning algorithm. We demonstrate that the classification algorithm outperforms the current standard of clinical care. This algorithm will ultimately be applied to translate the imaging data collected by PPG imaging and MSI into essential information for healthcare providers performing excision and grafting surgery.

METHODS

Photoplethysmography Imager

The PPG imager system consisted of a 10-bit monochromatic complementary metal-oxide–semiconductor camera (Nocturn XL, Photonis USA) that provides low dark noise and high dynamic range. The 10-bit analog-to-digital converter resolution offers a signal-to-noise ratio of 60 dB. The resolution of this imager was set to 1280×1040 (aspect ratio 5:4). The camera was mounted vertically and facing down to the object surface. A common field of view (FOV) of 20×16 cm was controlled for intersystem comparison. The exposure time of the camera was calibrated with a 95% reflectance reference standard (Spectralon SG3151; LabSphere Inc.; North Sutton, NH). To illuminate the tissue, four monochromatic and high-power light-emitting diode (LED) emitters (SFH 4740, OSRAM) were positioned in a 2×2 array mounted in the same plane as the sensor. The LED emitter array was placed with camera at 15 cm to the target surface. LED emitters were chosen because they provide an even illumination of the tissue in the camera's FOV (ie, the spatial intensity variation was less than 15%). The FOV of the camera was controlled by the optical lens and was slightly narrower than the illumination area.

Multispectral Imager

MSIs were collected by the Staring method using a filter-wheel camera (SpectroCam, Pixelteq; Largo, FL) equipped with eight unique optical band-pass filters between 400 and 1100 nm wavelengths. To select the most relevant filters for our system, we tested 22 unique filters identified in previous studies and performed wavelength selection data analysis using a technique called feature selection.[24] Wavelength filters with the following peak transmission were used in this study: 581, 420, 620, 860, 601, 680, 669, and 972 nm (filter widths were ±10 nm; Ocean Thin Films; Largo, FL). The system was calibrated using a 95% square reflectance standard (Spectralon SG3151; LabSphere Inc.; North Sutton, NH) to compensate for the different spectral response of the imaging sensor. The light source used was a 250-watt tungsten–halogen lamp (LowePro) equipped with a frosted glass diffuser to create a more even illumination profile within the imager's FOV. The system utilized a telescopic lens (Distagon T* 2.8/25 ZF-IR; Zeiss Inc.).

Swine Model

The methods used in this animal study were modified from Branski et al[25] and Gurfinkel et al.[26] Four adult Hanford swine weighing approximately 40 kg were acclimated before surgery. Surgery was performed under appropriate anesthesia. Initially, animals were sedated with Telazol (~2.2 mg/kg, internal medicine) and Xylazine (~0.44 mg/kg, internal medicine), then immediately intubated endotracheally and maintained using isoflurane (0.5–5% in 100% oxygen). The dorsolateral back area of each animal was closely clipped with electric clippers and shaved with a razor to remove hair. Deep partial-thickness burns were created proximal to the midline of the dorsal side of the pig. Injuries were generated using a spring-loaded brass rod heated to 100°C and pressed to the skin (pressure, 0.24 kg/m^2) for 60 seconds. The brass rod was 3.6 cm in diameter, and resulting wounds were of identical dimensions. A total of six injuries were generated on each pig to maintain spacing between wounds that would allow the use of healthy tissue adjacent to each circular burn as uninjured control tissue.

To calibrate the imaging devices to the proper excision depth, a standard model for sharp tangential excision was developed. This was accomplished by passing an electric dermatome (Zimmer; Model No.: 8821-06) set to 1.0 mm in depth (6.0 cm width) over the burn multiple times. We excised the deep partial-thickness burns in three passes of the dermatome to expose the wound bed. An excision was deemed successful if we had removed the tissue to a plane where punctate bleeding was present.

Data collection time points were (1) preinjury; (2) immediately post injury; (3–5) at each of the three excision depths (Figure 4). At each time point, we collected PPG images, MSI images, and physiologic data including heart rate, respiratory rate, and blood pressure. The healthy tissue adjacent to each circular burn was used as uninjured control tissue. After each tangential excision, we saved the excised tissue for histological assessment. Data were collected immediately after the burn injury with approximately 20 minutes between time points. Therefore, the initial excision occurred at approximately 20 minutes after the burn injury, and the final excision occurred approximately 80 minutes after burn injury.

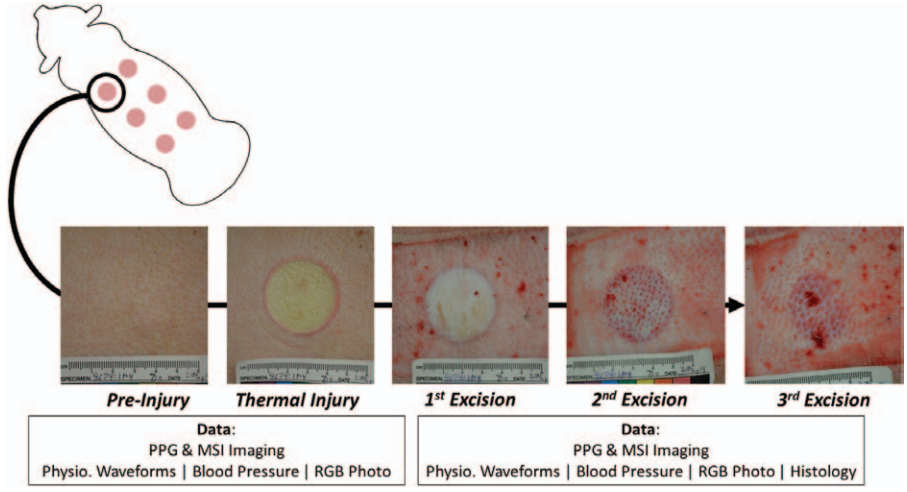

Figure 4. The steps involved in the deep partial-thickness porcine burn excision model. The five time points, color photographs, and data collection from each time point are depicted.

Identification of Viable Wound Bed

A histopathologist, who was blinded to the details of the study, determined the depth at which the viable wound bed was exposed using both histology and color photography. Histology was performed according to Gurfinkel et al.[5] Briefly, each tangentially excised tissue sample was fixed in 10% neutral buffered formalin and sent for processing and examination by a board certified histopathologist (Alizee Pathology, Thurmont, MD). One representative biopsy was taken from each sample and stained using hematoxylin and eosin. To determine at which tangential excision the viable wound bed was reached, the histopathologist identified the margins of the most severely burned areas of the thin slice of tissue, and morphometric analysis was used to find the depth of this burn (Figure 5). At each time point in the study, digital photographs of the burns were taken. A color reference strip was placed beside the wounds for standardization of color.

The severity of the burn injury was assessed by the histopathologist and graded as the coagulative zone or the zone of stasis. The coagulative zone represented the area where maximum damage has occurred. Histologically, this region was characterized by loss of cellular detail. The zone of stasis had decreased tissue perfusion as evidenced by vascular occlusion. In this region, collagen generally retains its structural integrity. However, there is some evidence of cellular necrosis, with pyknotic nuclei. This tissue zone is considered to have the potential to be salvaged during burn resection (Figure 6).

Image Processing and Statistics

All image processing and statistics were performed on MATLAB (v2013b). Data analysis for each imaging system is described as follows:

PPG Imager Data Analysis. PPG images are created according to Thatcher et al.[15] Briefly, a 27-second video of the burn was collected for each PPG image. For each pixel, the plethysmography waveform was identified (if present) by filtering the signal, performing a time-to-frequency conversion with a fast Fourier transform, and then identifying

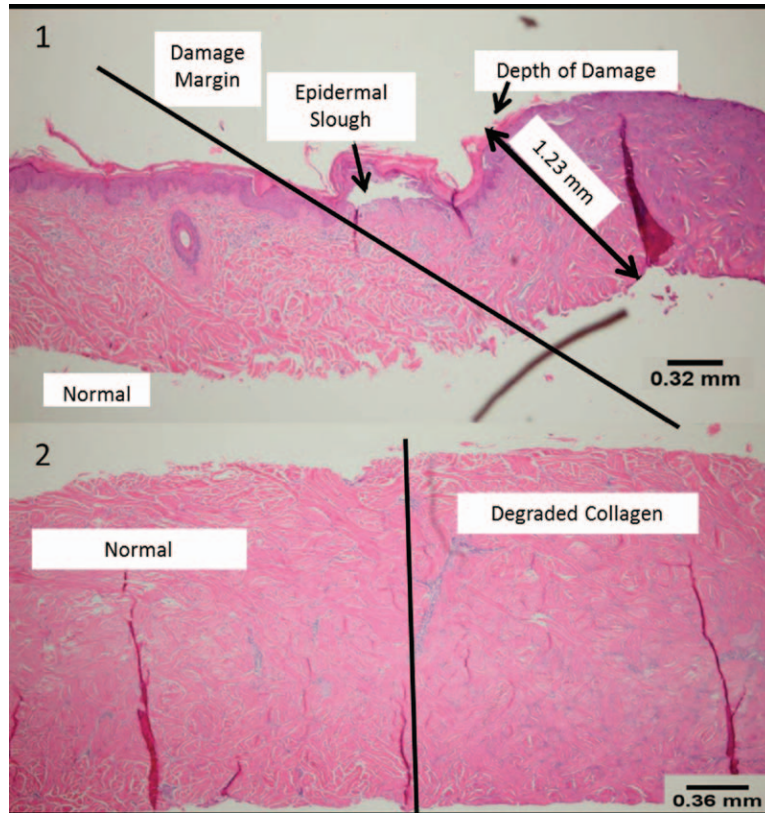

Figure 5. Histology of tangentially excised tissue specimens from a deep partial-thickness burn. Numbers indicate the order of excision from epidermis into the dermal layer. The most severely burned tissue lies in excision layer 1 (1). Tissue with minor burn effects lies in excision layer 2 (2), as seen by the similarities between normal and degraded collagen in that layer. Tissue in excision layer 3 is not shown and was determined to be without injury.

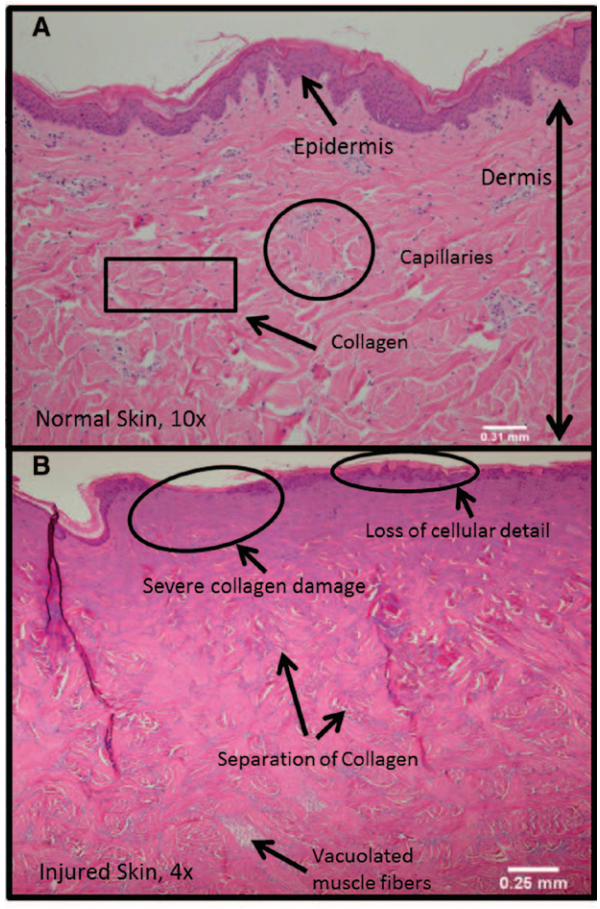

Figure 6. The average total depth was determined by measuring the extent of epidermal and dermal damage. A. Normal skin at a magnification of 10×. The epidermis, collagen, and capillaries have a distinct morphology. B. After thermal injury, the loss of epidermal detail, the separation of collagen, and the loss of collagen morphology. These characteristics define the extent of thermal injury and were used to indicate the coagulative zone and zone of stasis.

the signal strength at the frequency of the animal's heart rate. The final output images represented the relative amplitude of the plethysmography waveform at each pixel.

The introduction of noise into the PPG signal by the motion of the animal during respiration made initial analysis of PPI imaging difficult. We were able to reduce the influence of respiratory motion using a signal processing method called envelope extraction. To each pixel in the image, the signal was smoothed with a low pass filter to extract the envelope of the noisy signal. The noisy signal was then divided by its envelope to remove the dramatic motion spikes in the signal. The remaining clear signal demonstrated information that was then processed into the PPG image.

PPG imaging data were collected from six wounds and two animals totaling 12 burn injuries. From each wound, we imaged all five time points described in the animal model. From the PPG images of the burn injuries, we sorted pixels into three physiologic classes: healthy skin, burn injury, and viable wound bed. To compare the difference in PPG signal from tissue types, pixels from every image were sorted into their specific tissue type, based on the standard procedure of histology. These data were combined from both animals, summarized, and compared with analysis of variance. Multiple comparisons were performed using Tukey's honest significance test.

Classification Algorithm for Multispectral Imaging. To generate classified image outputs from the raw MSI data, a classification algorithm and a burn tissue spectral reference library were generated. To create a reference library, pixels of known physiology were labeled in our raw MSI data according to the histological findings.[27] Pixel labeling was performed by two technicians under supervision of an expert surgeon equipped with the histopathology results and the color photographs from each data collection time point. The color photographs could assist the expert to identify the location of punctate bleeding and viable vs nonviable tissue in the excised burn wounds. Sorting of pixels occurred on approximately 120 MSI images from 24 burns across four pigs, resulting in a reference library composed of approximately 4000 or more pixels per physiologic class.

The six burn tissue classes sorted into our reference library were as follows (Figure 7):

Healthy skin—Healthy skin was a common tissue present in almost all of our images and was chosen as a class to help determine the margins of burn injury.

Hyperemia—Hyperemia is one of the three zones of burn injury described by Jackson.[3] Vasculature in this area is vasodilated, and complete recovery of this tissue is to be expected.

Severe burn—Zone of coagulation where necrosis and irreversible burn injury has occurred. This tissue is not expected to heal spontaneously or support a skin graft because it was selected based on histological findings that indicate severe thermal damage.

Wound bed—Viable wound bed tissue that is expected to be ideal for applying skin grafts. It is white or pink in color with punctate bleeding, and histology of this tissue shows no thermal effects.

Some burn effects—Zone of stasis where the tissue has minor burn injury found at the margin between the severely burned tissue and the uninjured tissue.

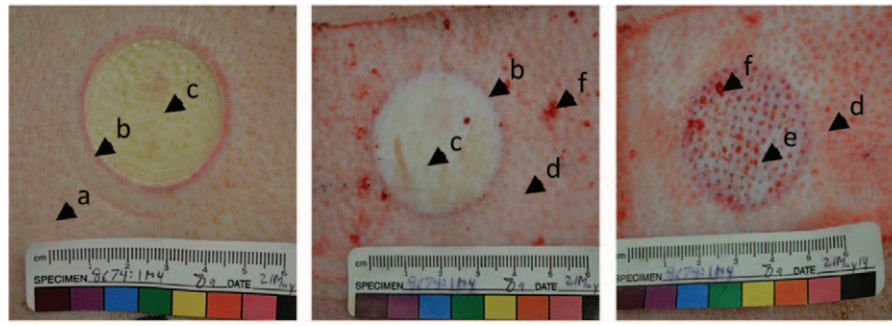

Figure 7. Location of the six tissue classes on color photographs of a burn injury at different excision depths: a, Healthy skin; b, hyperemia; c, severe burn; d, wound bed; e, some burn effects; f, blood pooled on the surface.

Blood—Large accumulations of blood on the surface of the tissue is part of this classification scheme. When tissue is classified as blood, the imager is expected to cue the surgeon to suction or clean the blood away and reimage this area.

A machine-learning algorithm to sort pixels into six different physiologic classes was developed based on the reference data generated in the previous step. We used quadratic discriminant analysis as our classifier algorithm. The algorithm's accuracy was determined as follows: once the pixels from each MSI image were sorted into their appropriate classes according to the histology, we trained our classification algorithm with 2000 pixels for each of the six classes across all 24 burn sites. Then, without replacement of the training pixels, we randomly selected a new set of 2000 per class as data to test the classification algorithm's efficiency using cross-validation. A confusion matrix was generated, and classification accuracy was calculated according to Sokolova and Lapalme.[28]

RESULTS

Burn Generation and Depth

Twenty-four deep partial-thickness burns were created on four minipigs. We found that 16 of 24 (67%) wounds had homogeneous wound areas with the pressure controlled burn rod. From each burn, three tangential excisions were taken, totaling 72 sections. Morphometric analysis was performed to quantify the consistency of the burn depth and the consistency of each tangential excision generated by the dermatome.

With each pass of the dermatome, the average thickness of excised tissue was 1.36 ± 0.16 mm (12% standard deviation; n = 72 excisions). We found that the average total depth of the burned tissue was 3.73 ± 0.58 mm (±16% standard deviation), and the depth of the Coagulative Zone was approximately 1.49 ± 0.59 mm (±39% standard deviation). The latter metric had the highest variance, which was likely related to the more subjective tissue changes used by the histopathologist to delineate this region from the region of some burn involvement (zone of stasis). The sectioning method we utilized for this experiment prevented us from measuring this depth accurately in our study. However, the skin on the dorsum of the minipig varies in depth and is reported to be 3.72 ± 0.11 cm in the Yorkshire swine, which makes the burns generated in this study very deep partial thickness.[29]

With the tangentially excised burn tissue, histology was performed to verify that we had reached the viable wound bed after three passes with the dermatome. An excision was deemed successful if we had removed the tissue to a point where punctate bleeding was present. In 24 of 24 injuries (100%), we removed the tissue to reveal even and punctate bleeding across the wound bed. This was confirmed by histology, which showed that all of the severely burned tissue was removed in three or fewer passes of the dermatome (Figure 8). Despite evidence of punctate bleeding, the histology demonstrated that in 8 of 24 injuries (33%), we had not completely removed all tissue with any burn effects. In such instances, we assumed that there was burn remaining in the wound bed with similar histological characteristics to the excised eschar from the above layer, and in all eight of these cases, this resulted in labeling the tissue as some burn effects for our classifier algorithm.

Photoplethysmography Imaging

We looked at the differences in the PPG signal from three tissues present in the images: healthy skin, burn injury, and wound bed tissue. We found a significant difference between the signal-to-noise ratio of the PPG signal from the burned tissues compared with the other two tissue types: healthy skin, 6.5 ± 3.4 dB; viable wound bed, 6.2 ± 4.1 dB; and burned tissue, 4.5* ± 2.5 dB (*$P < 0.05$).

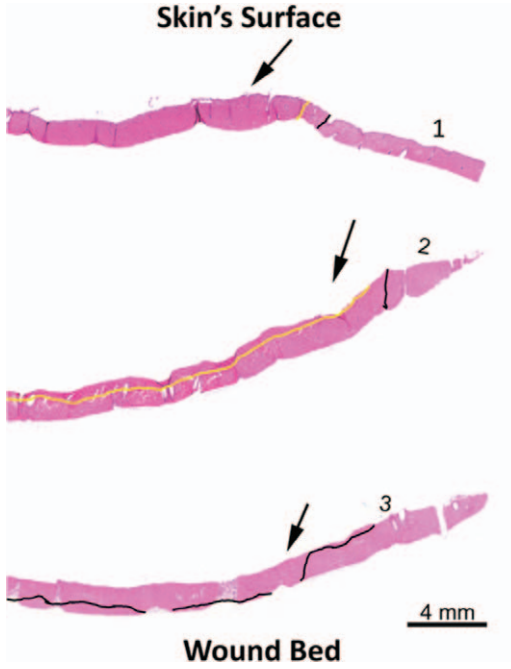

Figure 8. Complete histology sequence of tangentially excised tissue specimens from a deep partial-thickness burn. Numbers indicate the order of excision from epidermis into the dermal layer, and arrows indicate the most superficial aspect of each dermatome specimen. The most severely burned "coagulative zone" lies superficial to the yellow lines. The zone of stasis lies between the black and yellow lines. Tissue deep to the black lines was deemed to be normal.

We present one series of images from an injury to highlight the PPG signal changes throughout the depth of the burn (Figure 9). Initially, the PPG signal is relatively uniform across the uninjured skin. The signal dramatically decreases in the center of the image where the burn injury was created. As the first 1.0 mm layer of skin is removed, the burn tissue is still evident in the wound bed, and the lower relative PPG signal correlates to the presence of burn injury in the excised region. At a depth of approximately 2 to 3 mm (after the second cut), a PPG signal is identified in the burn wound bed, which indicates fresh blood flow through uninjured blood vessels beneath the deepest point of thermal injury.

Multispectral Imaging

From the labeled database of pixels selected under surgeon and histologist supervision, 2000 pixels randomly selected from all 24 burns were combined into a test data set. The test set was classified by the previously trained quadratic discriminant analysis algorithm and compared with their actual class labels to generate a confusion matrix (Table 1). This matrix shows the number of correct classifications across the diagonal in the center of the matrix. Incorrect classifications are in the off-diagonal elements. We found overall classification accuracy to be 86%. Blood expressed from the wound bed could be classified by our algorithm with 92% success rate, the highest accuracy of the six classes. The other five classes were classified with similar rates of accuracy with "severe burn" having the lowest classification accuracy at 81%. The confusion matrix demonstrates that a common inaccuracy was the misclassification of severely burned tissue as healthy skin and healthy skin as severe burn. Also, we find that hyperemic tissue is often misclassified as blood and vice versa.

The classified MSI image outputs demonstrate the location of the burn and its margins well (Figure 10). MSI could surely identify the viable wound bed as we cut deeper into the burn area with the dermatome. Again, the misclassification of pixels mentioned previously is seen in these images. The spatial representation shows that errors are not typically random, but rather they occur in certain areas of the image with higher frequency. For example, much of the wound bed was classified as healthy skin in error only in the top portion of the first excision image in Figure 10.

For a burn that contained different burn depths within the same injury (a common clinical scenario), the MSI image results could identify the more severely burned areas (Figure 11). This was the case for the time points that occurred immediately after injury and during the excision process.

DISCUSSION

The animal model provided a suitable method to mimic burn surgical technique of sharp tangential excision in a reproducible manner. Burn tissue was strong enough to withstand shear stress from the dermatome despite degradation of structural proteins. Burn resection scenarios achieved in this model included under excision, over excision, and properly excised wound beds. Although the dermatome was set to 1.0 mm thickness, the average thickness of the excision was slightly thicker. This can be attributed to the downward force applied by the technician operating the dermatome. An increased force was used to ensure the tissue was removed intact, and this likely resulted in increased excision thickness by compressing the tissue as it was removed.

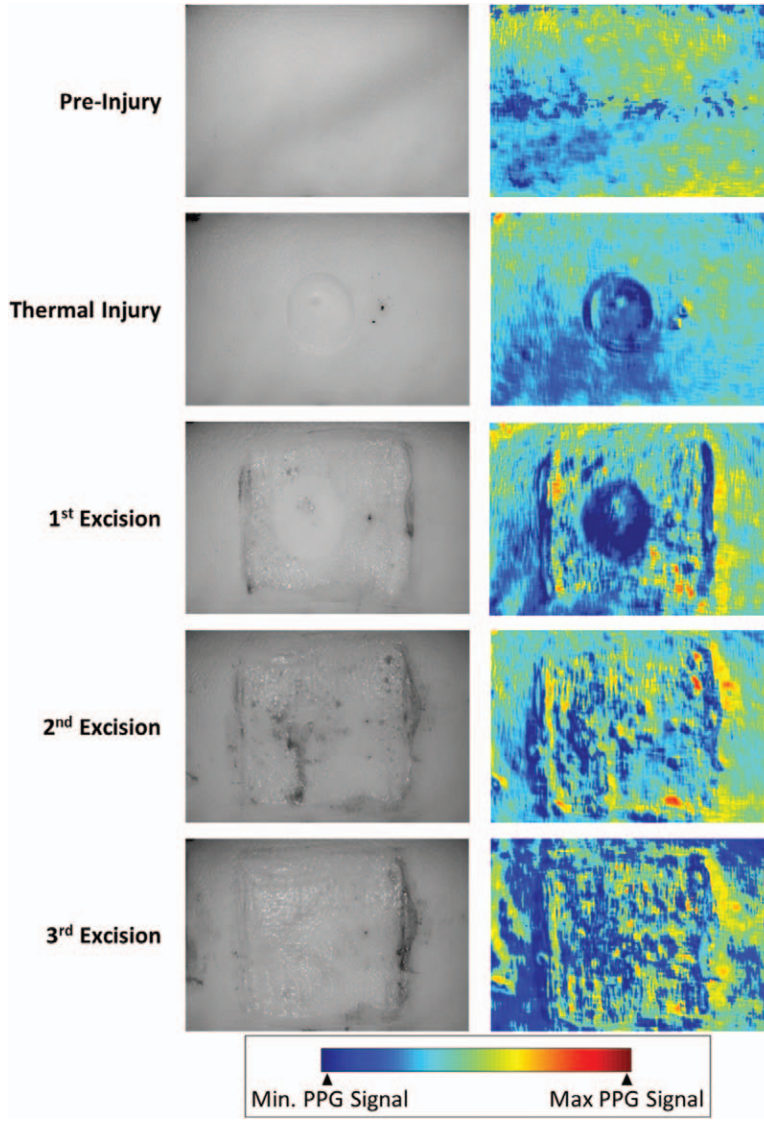

Figure 9. (Left) Greyscale reference images, and (Right) photoplethysmography (PPG) imaging results from serial tangential excision of a deep partial-thickness burn. In the thermal injury and first excision time points, burn tissue is evident by the lower relative PPG signal. In the second excision and third excision time points, there is PPG signal in the wound bed. This indicates blood flow in the tissue and reduced or absent thermal injury at this depth.

Results from the PPG imaging data demonstrate that burned tissue has significantly less PPG signal compared with healthy tissue. From a clinical standpoint, this means that a suspected burn injury can be identified with the assistance of PPG imaging technology. As a surgeon excised tissue, they could expect a corresponding increase in PPG imaging signal as they removed necrotic tissue to expose a perfused wound bed. When the signal reached a PPG intensity characteristic of viable tissue, a PPG imaging device would indicate to a surgeon that there is adequate blood flow in the wound bed and that the tissue would support a graft. Further research will be necessary to determine whether an automatic threshold value of the PPG signal can be identified and used to accurately separate viable from nonviable tissue.

Results from MSI imaging are also promising. With the eight wavelengths used in this study, we arrived at an average of 86% accuracy in classification of various tissue classes. The six tissue classes chosen for this analysis were selected after discussion with burn surgeons, analysis of preliminary MSI data generated in our laboratory, and attempts to adhere to the classic zones of burn injury described by Jackson.[3] However, we realize that these six specific tissue classes may not relevantly translate to a clinical setting. These classes

Table 1. Multispectral Imaging Confusion Matrix and Classification Accuracy

		Actual State of Tissue Under Test							
		Healthy Skin	Wound Bed	Less Severe Burn	Severe Burn	Blood	Hyperemia	Accuracy (%)	Average Effectiveness
Classification result	Healthy skin	1216	291	34	948	31	101	82	86%
	Wound bed	211	1264	314	226	0	14	87	
	Less severe burn	48	132	1175	21	5	250	89	
	Severe burn	485	294	103	761	0	199	81	
	Blood	9	7	46	2	1061	13	92	
	Hyperemia	31	12	328	42	903	1423	84	

can be altered for applications in humans, and clinical trials will be necessary to determine relevant tissue classifications for clinical application.

Despite its high accuracy, MSI images contain some areas of misclassified tissue. For instance, in some cases, the healthy skin was classified as burn tissue (Figure 10). Future work is necessary to continue to improve the accuracy of MSI to a level tolerable to a clinician. Nevertheless, the initial application of MSI in tissue classification suggests that this technology has significant potential to improve clinical decision making. We do not believe that this technology can replace clinical judgment—rather it is expected to be a clinical assist tool, and an expert clinician is needed to determine the final surgical plan.

We have presented two imaging methods that perform similarly in identifying viable from nonviable tissues. However, the two techniques are fundamentally different in the physiologic characteristics that they measure. PPG imaging can identify viability by measuring the dynamic changes in tissue blood flow, which are only present in living tissue, and blood flow in the skin is amenable to physician interpretation. However, PPG imaging is dependent on adequate blood pressure and is highly sensitive to motion of the patient. MSI is very rapid and much less sensitive to patient motion, and a variety of tissue types can be identified with only a few key measurements. However, the system's wavelengths must be determined experimentally, and the algorithm is based on previously collected reflectance tissue data that must be used for algorithm training before use on a patient. Both imaging modalities may be affected by skin pigmentation differences and the presence of tattoo ink.[30] The hardware to perform both imaging types is available off-the-shelf at relatively low costs with high durability.

The fusion of these technologies into a single classification image is currently under development. Features calculated from the PPG data can be combined with the reflectance spectrum data using the same machine-learning techniques already established for MSI data analysis to further increase classification accuracy. Because both PPG and MSI raw data can be collected with the same optical hardware, it is a matter of statistical analysis to determine the salient features from each system to include in the classifier equation. Although MSI alone can effectively identify the margins of the burn, we believe the dynamic blood-flow information from the PPG signal will combine with the reflectance data to include critical tissue viability information, increasing classification accuracy over one or the other technology alone.

The proper classification of burn wounds during excision and grafting is essential to optimizing care for burn patients. The current standard of care for burn tissue classification is the clinical judgment of experienced burn surgeons via direct visualization. Typically, burned tissue is excised in layers until the surgeon can visualize a viable wound bed as suggested by the presence of punctate bleeding from capillaries.[2] This technique, however, has never been clinically validated, and up to half of excised tissue is actually viable and unnecessarily removed.[5,31] This suggests that relying on visualization of punctate bleeding as a stopping point during burn resection results in excessive excision, and, therefore, a method to identify viable tissue earlier in the process would spare a significant amount of viable tissue. Both PPG imaging and MSI have shown promise in this study to characterize viable tissue accurately without reliance on visualizing surface punctate bleeding because the light collected and measured by these technologies penetrates through the tissue surface before being scattered and returning to the camera. This information collected below the surface of the tissue is not available to the naked eye, so PPG imaging and MSI should be able to identify appropriate stopping points during excision earlier than visualization. Although the data from this study suggest feasibility for clinical application, our study has some limitations. The acute nature of our experiment limits the interpretation of these results to a very acute

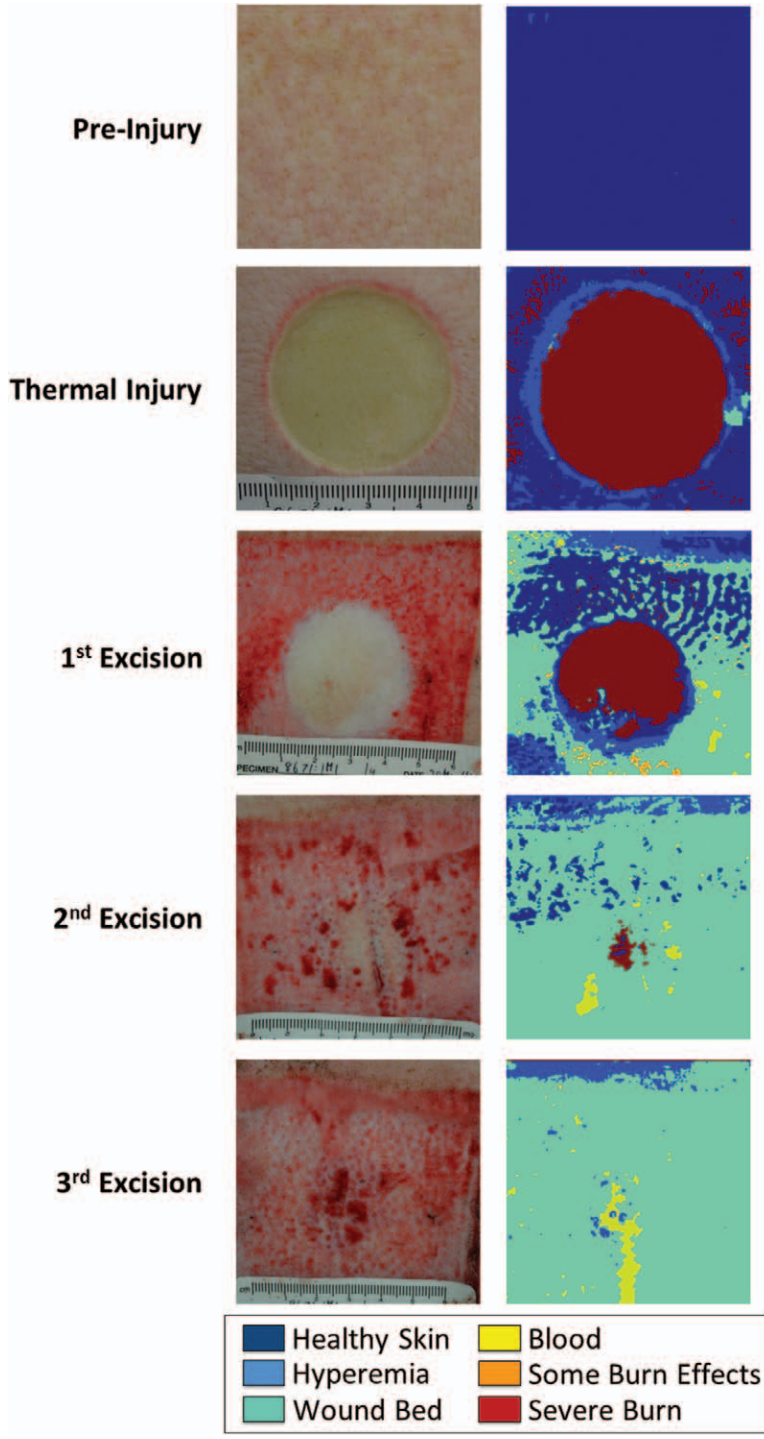

Figure 10. Multispectral images from the serial tangential excision of a deep partial-thickness burn. The presence of severe burn decreases as more layers of skin are removed. At the second excision, the burn is nearly excised and is completely removed at the third excision. Some errors are present, notably in the first excision where healthy wound bed is classified as healthy skin. Error can be decreased through algorithm and hardware improvements, such as selecting more effective wavelengths.

burn setting. In our experiment, the inflammatory response that follows hours to days after burn injuries was not given time to fully manifest, and burn progression would not be completed after such a short duration between burn injury and data collection.[32,33] Therefore, the tissue that we have deemed

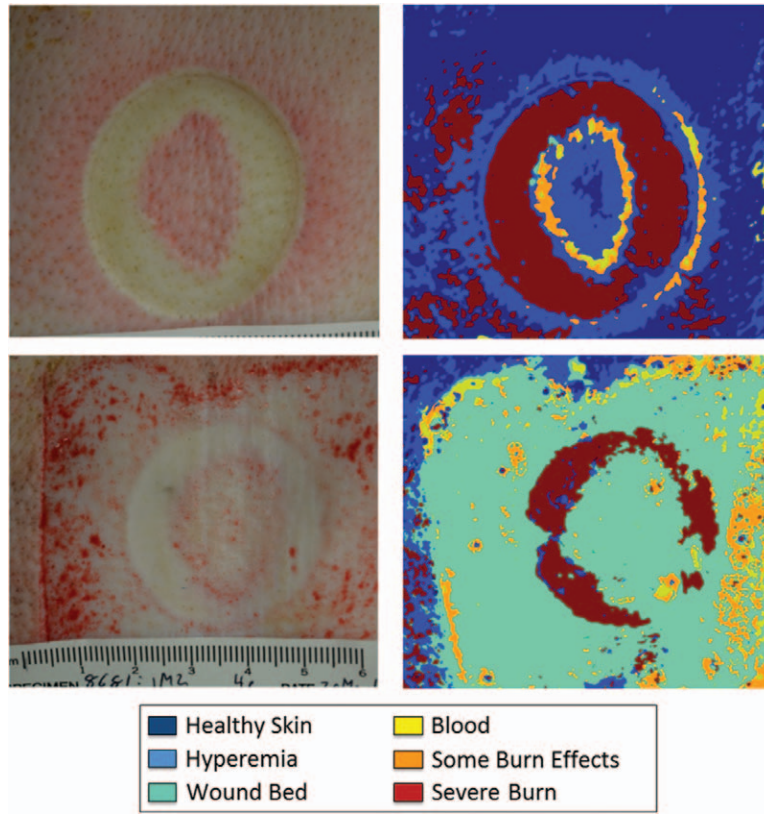

Figure 11. The effectiveness of the multispectral imaging technique can be observed in this heterogeneous burn. The internal portion of this injury was burned less severely than the outer ring, confirmed by histology. Burns of heterogeneous depth are common in the clinical setting. A burn such as this may be presented to the surgeon who must determine whether the tissue needs surgery (top). During surgery, the surgeon encounters burns of nonuniform depth. These images can cue the surgeon as to where more burn injury must be removed and where viable wound bed is already reached (bottom).

viable according to histology may have eventually progressed with conversion to nonviable tissue given additional time. Future studies are planned to assess the time of excision in relation to burn injury as an important variable. Also, the clinical viability of a wound bed can only be confirmed by a study following the success of grafts after excision. In general, these technologies will be applicable to the human setting only following carefully planned clinical trials.

Applicability to Practice

Proper wound bed preparation during sharp tangential excision is important to prevent complications. Incomplete removal of eschar results in placement of grafts on devitalized tissue causing poor graft uptake and increased risk for infection.[8,34] Conversely, excision past the margin between nonviable and viable skin risks loss of the skin's regenerative capacity. Recent animal and human investigations have demonstrated that, if sufficient viable dermis is left intact after enzymatic debridement of partial-thickness burns, the remaining dermis can epithelialize spontaneously, which reduces autografting and donor sites.[31,35] Similarly limiting tangential excisional debridement to only the removal of injured tissue may result in the same benefit.

In addition to performing the technical aspects of the procedure, the surgeon must be able to dictate the proper fluid and blood management perioperatively.[36] Furthermore, timing is critical, as patients who undergo excision for wounds after only 48 hours lose twice the amount of blood when compared with similar patients who receive surgery 24 hours earlier.[37] Finally, multiregion burns that vary in depth over the total burn area further complicate provision of burn care.[38] Excision and grafting of these burns is challenging to plan to ensure maximal removal of unviable tissue with minimal excision of remaining viable skin.

Even determining whether the patient requires surgery can be challenging to burn specialists, as the accuracy of initial visual burn depth assessment by experienced surgeons has been reported to be 60 to

80% accurate for decades.[12] Although the focus of this article is not on initial burn depth assessment, it is important to note that both PPG imaging and MSI may be utilized to assess burn depth using the same strategies as for identifying viable wound beds during surgery.[22] Because inexperienced surgeons are even less accurate (approximately 50%) at initial burn depth assessment, these technologies would be particularly useful during disaster scenarios when burn specialists may be overwhelmed with patients.[6]

The ideal solution would be a clinical device that can identify regions that must be excised, determine the proper depth of excision, and monitor vitals to guide therapeutic management of the patient. Further requirements for clinical adaption would be an increase in diagnostic accuracy, accommodation of realistic patient conditions, and provision of useful data immediately to the treatment team. Furthermore, a solution could be employed based on these imaging techniques to aid nonspecialists in a situation where burn specialists were overwhelmed with patients, such as in a mass casualty event.

As previously discussed, several imaging modalities have been proposed as potential solutions to this problem. To date, most technologies have proven impractical in clinical practice for a variety of reasons. Some technologies are less accurate than the unaided clinical judgment of surgeons. Other solutions require patients to lie immobilized for prolonged periods, have data acquisition times on the order of days, or require invasive procedures for accurate diagnosis. Clinical tools with these limitations have not been readily adopted by healthcare providers.[39]

Initial investigations into MSI and PPG imaging, including the experiments outlined in this manuscript, have shown promise that these technologies may in fact meet these requirements to improve burn care. By working to translate these technologies into clinical tools that can be utilized at the bedside, outcomes in quality-of-life metrics can be improved for burn victims.

ACKNOWLEDGMENTS

This research was supported in part by the Biomedical Advanced Research and Development Authority (BARDA). We would like to acknowledge Professor Steven E. Wolf, MD, for his expert advice in burn care.

REFERENCES

1. Sterling J, Heimbach D, Gibran N. 7 Trauma and thermal injury: 15 management of the burn wound. In ACS: principles and practice. Hamilton, Ontario: Decker Intellectual Properties; 2010, p. 1–13.
2. Orgill DP. Excision and skin grafting of thermal burns. N Engl J Med 2009;360:893–901.
3. Jackson DM. [The diagnosis of the depth of burning]. Br J Surg 1953;40:588–96.
4. Devgan L, Bhat S, Aylward S, Spence RJ. Modalities for the assessment of burn wound depth. J Burns Wounds 2006;5:e2.
5. Gurfinkel R, Rosenberg L, Cohen S, Barezovsky A, Cagnano E, Singer A. Histological assessment of tangentially excised burn eschars. Can J Plastic Surg 2010;18:e33–36.
6. Jaskille AD, Shupp JW, Jordan MH, Jeng JC. Critical review of burn depth assessment techniques: part I. Historical review. J Burn Care Res 2009;30:937–47.
7. Heimbach DM, Afromowitz MA, Engrav LH, Marvin JA, Perry B. Burn depth estimation–man or machine. J Trauma 1984;24:373–8.
8. Tenenhaus M, Rennekampff HO. Burn surgery. Clin Plast Surg 2007;34:697–715.
9. Pape S, Skouras C, Byrne P. An audit of the use of laser Doppler imaging (LDI) in the assessment of burns of intermediate depth. Burns 2000; 27: 233–9.
10. Mo W, Mohan R, Li W, et al. The importance of illumination in a non-contact photoplethysmography imaging system for burn wound assessment. In: *Proceedings of SPIE 9303, photonic therapeutics and diagnostics XI, 93030M*, San Francisco, CA, 2015.
11. Kaiser M, Yafi A, Cinat M, Choi B, Durkin A. Noninvasive assessment of burn wound severity using optical technology: a review of current and future modalities. Burns 2011; 37:377–386.
12. Jaskille AD, Ramella-Roman JC, Shupp JW, Jordan MH, Jeng JC. Critical review of burn depth assessment techniques: part II. Review of laser Doppler technology. J Burn Care Res 2010;31:151–7.
13. Severinghaus J, Honda Y. History of blood gas analysis. VII. Pulse oximetry. J Clin Monitor 1987;3:135–8.
14. Webster J, Design of pulse oximeters, medical science series. New York and Bristol: Institute of Physics Publishing; 1997.
15. Thatcher J, Plant K, King D, Block K, Fan W, DiMaio J. Dynamic tissue phantoms and their use in assessment of a non-invasive optical plethysmography imaging device. In: SPIE, Smart biomedical and physiological sensor technology XI;9107:18-1–18-18.
16. Hu S, Peris V, Echiadis A, Zheng J, Shi P. Development of effective photoplethysmographic measurement techniques: from contact to non-contact and from point to imaging. Conf Proc IEEE Eng Med Biol Soc 2009: 6550–6553.
17. Li Q, He X, Wang Y, et al. Review of spectral imaging technology in biomedical engineering: achievements and challenges. J Biomed Optics 2013;18:100901.
18. Nguyen J, Crouzet C, Mai T, et al. Spatial frequency domain imaging of burn wounds in a preclinical model of graded burn severity. J. Biomed. Optics 2013;18: 66010.
19. Anselmo VJ, Zawacki BE. Multispectral photographic analysis. A new quantitative tool to assist in the early diagnosis of thermal burn depth. Ann Biomed Eng 1977;5:179–93.
20. Afromowitz MA, Callis JB, Heimbach DM, DeSoto LA, Norton MK. Multispectral imaging of burn wounds: a new clinical instrument for evaluating burn depth. IEEE Trans Biomed Eng 1988;35:842–50.
21. Eisenbeiss W, Marotz J, Schrade JP. Reflection-optical multispectral imaging method for objective determination of burn depth. Burns 1999;25:697–704.
22. King D, Li W, Squiers J, et al. Surgical wound debridement sequentially characterized in a porcine burn model with multispectral imaging. Burns 2015;41:1478–87.
23. Li W, Mo W, Zhang X, et al. Outlier detection and removal improves accuracy of machine learning approach to multispectral burn diagnostic imaging. J Biomed Opt 2015;20:121305.

24. Liu H, Yu L. Toward integrating feature selection algorithms for classification and clustering. IEEE Trans Knowl Data Eng 2005;17: 491–502.
25. Branski LK, Mittermayr R, Herndon DN, et al. A porcine model of full-thickness burn, excision and skin autografting. Burns 2008;34:1119–27.
26. Gurfinkel R, Singer AJ, Cagnano E, Rosenberg L. Development of a novel animal burn model using radiant heat in rats and swine. Acad Emerg Med 2010;17:514–520.
27. Li W, Mo W, Zhang X, et al. Burn injury diagnostic imaging device's accuracy improved by outlier detection and removal. In: Proceedings of SPIE 9472, algorithms and technologies for multispectral, hyperspectral, and ultraspectral imagery XXI, Baltimore, MD;2015:947206.
28. Sokolova M, Lapalme G. A systematic analysis of performance measures for classification tasks. Inf Process Manage 2009; 45:427–37.
29. Sumena K, Lucy L, Chungath J, Ashok N, Harshan K. Morphology of the skin in large white Yorkshire pigs. Indian J Anim Res 2010; 44: 55–57.
30. Your heart rate. What it means, and where on Apple watch you'll find it. May 30, 2015. [Online]. Available: https://support.apple.com/en-ca/HT204666; accessed 31 May 2015.
31. Rosenberg L, Krieger Y, Bogdanov-Berezovski A, Silberstein E, Shoham Y, Singer A. A novel rapid and selective animatic debridement agent for burn wound management: a multicenter RCT. Burns 2014:466: 466–74.
32. Gauglitz GG, Song J, Herndon DN, et al. Characterization of the inflammatory response during acute and post-acute phases after severe burn. Shock 2008;30:503–7.
33. Schmauss D, Rezaeian F, Finck T, Machens HG, Wettstein R, Harder Y. Treatment of secondary burn wound progression in contact burns-a systematic review of experimental approaches. J Burn Care Res 2015;36:e176–89.
34. Church D, Elsayed S, Reid O, Winston B, Lindsay R. Burn wound infections. Clin Microbiol Rev 2006;19:403–34.
35. Singer A, Taira B, Anderson R, McClain S, Rosenberg L. The effects of rapid enzymatic debridement of deep partial-thickness burns with Debrase on wound reepithelialization in swine. J Burn Care Res 2010;31: 795–802.
36. Bak Z, Sjöberg F, Eriksson O, Steinvall I, Janerot-Sjoberg B. Hemodynamic changes during resuscitation after burns using the Parkland formula. J Trauma 2009;66:329–36.
37. Desai MH, Herndon DN, Broemeling L, Barrow RE, Nichols RJ Jr, Rutan RL. Early burn wound excision significantly reduces blood loss. Ann Surg 1990;211:753–9; discussion 759–62.
38. Lee J, Dibildox M, Jimenez C, et al. Operative wound management. In: *Total burn care*. 4th ed. Philadelphia, Pennsylvania: Elsevier Inc.; 2012.
39. Resch TR, Drake RM, Helmer SD, Jost GD, Osland JS. Estimation of burn depth at burn centers in the United States: a survey. J Burn Care Res 2014;35:491–7.